JOURNAL OF GUIDANCE, CONTROL, AND DYNAMICS
Vol. 21, No. 6, November–December 1998

Passive Control of Displaced Solar Sail Orbits

Colin R. McInnes*
University of Glasgow, Glasgow, Scotland G12 8QQ, United Kingdom

An analysis of the linear stability and control of families of displaced solar sail orbits is presented. Three families of orbits are reviewed along with their linear stability characteristics. It is then shown that the unstable subfamilies of orbits that exist are controllable using state feedback to the sail attitude. However, a more useful result is presented that demonstrates that linear stability can be achieved if the sail attitude is fixed relative to the sun-sail line. Such an attitude can be achieved by passive means by a suitable choice of sail shape. Therefore, the subfamilies of unstable orbits can in principle be stabilized by fully passive means. Such passive control is clearly useful for simplifying station-keeping on such orbits.

Nomenclature

$\boldsymbol{a}, a$ = solar radiation pressure acceleration
$\boldsymbol{C}$ = controllability matrix
g = feedback gains
$\boldsymbol{K}$ = input matrix
$\boldsymbol{L}$ = open-loop system matrix
$\boldsymbol{M}$ = gravity gradient matrix
$\boldsymbol{N}, \boldsymbol{n}$ = radiation gradient matrix, sail unit normal vector
o = evaluated along nominal orbit
$\boldsymbol{P}$ = passive control system matrix
$\boldsymbol{r}, r$ = sail position vector, sun-sail distance
$\boldsymbol{S}, S$ = gyroscopic matrix, boundary surface
U = modified potential function
V = gravitational potential function
$\boldsymbol{x}$ = state vector
z = sail vertical coordinate
α = sail pitch angle
β = sail lightness number
γ = sail elevation angle
$\boldsymbol{\delta}$ = position perturbation
η = vertical perturbation
λ = variational equation eigenvalue
μ = product of gravitational constant and solar mass
ξ = radial perturbation
ρ = sail radial coordinate
σ = sail loading
ψ = azimuthal perturbation
$\boldsymbol{\omega}, \tilde{\omega}$ = angular velocity, Keplerian orbit angular velocity
$\hat{}$ = unit vector

I. Introduction

DISPLACED solar sail orbits have previously been investigated by a number of authors, who detailed the properties of large families of sun-centered orbits.[1–7] These families are circular solar sail orbits that are displaced out of the ecliptic plane using a component of the solar radiation pressure force exerted on the sail. Displaced orbits are unlike other solar sail orbits in that they can be considered as equilibrium solutions to the equations of motion when viewed from a rotating frame of reference. Initial investigations considered the conditions for displaced orbits for an ideal, perfectly reflecting solar sail.[1–4] Then, further analysis considered a more realistic solar sail model with nonperfect reflectivity.[5–7] It has also been found that some families of displaced orbits are unstable or have regions of instability, which clearly limits their potential usefulness for mission applications.[2–4]

In this paper the families of displaced orbits and their linear stability characteristics are first reviewed. Then, it is demonstrated that the unstable orbits are, in general, controllable using feedback to the sail attitude alone. Using this result, an active control scheme is developed, which provides linear stability. As an alternative, a passive control scheme is investigated, which renders all families of orbits linearly stable. The passive control scheme requires that the sail attitude is fixed relative to the sun as the sail is perturbed. This requirement can be achieved, for example, by designing the sail to be slightly conical in shape, with the apex of the cone directed toward the sun. A suitable offset of the center of mass from the center of pressure then fixes the sail at some desired attitude relative to the sun. Because of its inherent simplicity, the passive control scheme appears to be an attractive and interesting means of orbit stabilization.

Received Sept. 24, 1997; revision received April 12, 1998; accepted for publication May 12, 1998.

*Reader, Department of Aerospace Engineering.

II. Displaced Orbit Solutions

An idealized, perfectly reflecting solar sail will be considered at position $\boldsymbol{r}$ in a frame of reference rotating with angular velocity $\boldsymbol{\omega}$, as shown in Fig. 1. The sail orientation is defined by the unit vector $\boldsymbol{n}$ normal to the sail surface, which is fixed in the rotating frame of reference. The sail performance is characterized by the sail lightness number β, which is defined as the ratio of the solar radiation force to solar gravitational force exerted on the sail. Because both solar gravity and solar radiation pressure (except close to the sun[8]) have an inverse square variation, the sail lightness number is a constant. It can be shown that the sail lightness number[9] is related to the sail loading (mass per unit area) σ by $\beta = 1.529/\sigma$ (gm^{-2}) (see Appendix) so that a high-performance sail will have a low mass per unit area. In addition, because the sail orientation is fixed in the rotating frame, the solar sail must rotate once per orbit with respect to an inertial frame of reference. The equation of motion for the solar sail in the rotating frame of reference may be written as

$$\frac{\mathrm{d}^2\boldsymbol{r}}{\mathrm{d}t^2} + 2\boldsymbol{\omega} \times \frac{\mathrm{d}\boldsymbol{r}}{\mathrm{d}t} + \boldsymbol{\omega} \times (\boldsymbol{\omega} \times \boldsymbol{r}) = \boldsymbol{a} - \nabla V \tag{1}$$

where the terms on the left in Eq. (1) represent the kinematic, coriolis, and centripetal accelerations, respectively. These accelerations are equated to the solar radiation pressure acceleration $\boldsymbol{a}$ and solar gravitational acceleration $-\nabla V$ exerted on the sail. The solar radiation-pressure acceleration and the two-body gravitational potential V are given by

$$\boldsymbol{a} = \beta(\mu/r^2)(\hat{\boldsymbol{r}} \cdot \boldsymbol{n})^2 \boldsymbol{n} \tag{2a}$$

$$V = -(\mu/r) \tag{2b}$$

It can be seen from Eq. (2a) that the sail acceleration is a function of its orientation relative to the sun line. This is due to the variation of the projected sail area and the variation of the component of force normal to the sail surface as the sail is rotated. Because the solar radiation-pressure acceleration can never be directed sunwards, the constraint $\hat{\boldsymbol{r}} \cdot \boldsymbol{n} \geq 0$ is imposed.

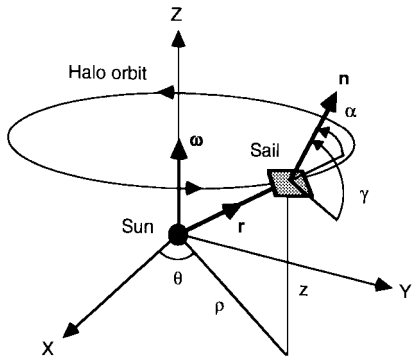

Fig. 1 Sun-centered rotating frame of reference.

It is now noted that the centripetal term in Eq. (1) is conservative, and so may be written in terms of a scalar potential Φ defined such that

$$\Phi = -\tfrac{1}{2}|\boldsymbol{\omega} \times \boldsymbol{r}|^2 \tag{3a}$$

$$\nabla\Phi = \boldsymbol{\omega} \times (\boldsymbol{\omega} \times \boldsymbol{r}) \tag{3b}$$

A new modified potential $U = V + \Phi$ will now be defined so that a reduced equation of motion is obtained, viz.,

$$\frac{\mathrm{d}^2\boldsymbol{r}}{\mathrm{d}t^2} + 2\boldsymbol{\omega} \times \frac{\mathrm{d}\boldsymbol{r}}{\mathrm{d}t} + \nabla U = \boldsymbol{a} \tag{4}$$

In the rotating frame of reference an equilibrium solution is required so that the first two terms of Eq. (4) must vanish. Because the vector $\boldsymbol{a}$ is oriented in direction $\boldsymbol{n}$, taking the vector product of $\boldsymbol{n}$ with Eq. (4) it is found that

$$\nabla U \times \boldsymbol{n} = 0 \Rightarrow \boldsymbol{n} = \varepsilon\nabla U \tag{5}$$

where ε is an arbitrary scalar multiplier. Using the normalization condition $|\boldsymbol{n}| = 1$, ε is then identified as $|\nabla U|^{-1}$ so that the required sail attitude is defined simply by

$$\boldsymbol{n} = \nabla U/|\nabla U| \tag{6}$$

Because the solar sail is to have uniform azimuthal motion, there can be no component of the vector $\boldsymbol{n}$, and so of $\boldsymbol{a}$, in the azimuthal direction. Therefore, $\boldsymbol{n}$ is contained in the plane spanned by $\hat{\boldsymbol{r}}$ and $\boldsymbol{\omega}$ so that the sail attitude may be described solely in terms of the pitch angle α between $\boldsymbol{n}$ and $\hat{\boldsymbol{r}}$, as shown in Fig. 1. Taking vector and scalar products of Eq. (6) with $\hat{\boldsymbol{r}}$, it is found that

$$\tan\alpha = \frac{|\hat{\boldsymbol{r}} \times \nabla U|}{\hat{\boldsymbol{r}} \cdot \nabla U} \tag{7}$$

Similarly, the required sail lightness number is obtained by taking a scalar product of Eq. (4) with $\boldsymbol{n}$, again requiring an equilibrium solution, viz.,

$$\beta = \frac{r^2}{\mu}\frac{\nabla U \cdot \boldsymbol{n}}{(\hat{\boldsymbol{r}} \cdot \boldsymbol{n})^2} \tag{8}$$

General functions for the sail attitude and sail lightness number have now been obtained in terms of the two-body rotating potential function U. For a given orbit period, orbit radius, and displacement distance, the solar sail pitch angle and lightness number required for a displaced orbit then can be obtained.

If the set of cylindrical coordinates (ρ, θ, z) shown in Fig. 1 are now used, the rotating two-body potential function may be written as

$$U = -\left[\tfrac{1}{2}\rho^2\omega^2 + (\mu/r)\right] \tag{9}$$

where the angular velocity ω is related to the orbit period T by $\omega = 2\pi/T$. Evaluating the potential gradient in Eqs. (7) and (8) it is found that

$$\tan\alpha = \frac{(z/\rho)(\omega/\tilde{\omega})^2}{(z/\rho)^2 + [1 - (\omega/\tilde{\omega})^2]}, \qquad \tilde{\omega}^2 = \frac{\mu}{r^3} \tag{10a}$$

$$\beta = \left[1 + \left(\frac{z}{\rho}\right)^2\right]^{\frac{1}{2}} \frac{\{(z/\rho)^2 + [1 - (\omega/\tilde{\omega})^2]^2\}^{\frac{3}{2}}}{\{(z/\rho)^2 + [1 - (\omega/\tilde{\omega})^2]\}^2} \tag{10b}$$

where $\tilde{\omega}$ is the orbital angular velocity of a circular Keplerian orbit of radius r. For convenience, the parameter μ may now be chosen to be unity so that the unit of distance becomes the astronomical unit (AU) and the unit of nondimensional time becomes $(2\pi)^{-1}$ years. In addition, it can be seen that the preceding expressions are independent of the azimuthal angle θ. Therefore, for fixed-sail lightness numbers, Eq. (10b) defines nested surfaces of revolution about the z axis.

III. Orbit Families

Type I

For this family of orbits the solar sail orbit period is chosen to be that of a Keplerian orbit of radius equal to the sun-sail distance r so that $\omega = \tilde{\omega}$. Surfaces of corotation (equal orbital period) are then defined by spheres of constant radius. Substituting for this functional form of ω, the required sail pitch angle and sail lightness number are obtained as

$$\tan\alpha = \rho/z \tag{11a}$$

$$\beta = [1 + (\rho/z)^2]^{\frac{1}{2}} \tag{11b}$$

It can be seen from Eqs. (11) that the sail is always oriented perpendicular to the ecliptic plane. Therefore, the constraint $\hat{\boldsymbol{r}} \cdot \boldsymbol{n} \geq 0$ is always satisfied, and the extent of the family of orbits in the ρ–z plane is not bounded. In addition, it can be seen that for any combination of orbit radius and displacement distance a sail lightness number of greater than unity is always required. It is noted that owing to the symmetry of the problem the axis of the displaced orbit need not be normal to the ecliptic plane. A displaced orbit may be established about any axis passing through the origin so that off-axis orbits, inclined to the ecliptic, are possible.

Type II

For this family of orbits, the solar sail orbit period will be chosen to be some fixed value for all values of orbit radius and displacement. For example, a family of Earth-synchronous 1-year orbits may be generated by setting $\omega = 1$ in Eq. (10b). A section of the surfaces of equal sail lightness number generated by Eq. (10b) are shown in Fig. 2 along with the required direction of the sail normal vector $\boldsymbol{n}$. In addition, the equivalent sail loading values are listed in Table. 1. It can be seen in Fig. 2 that topologically the full three-dimensional surfaces form a family of nested tori for $\beta < 1$ and nested cylinders for $\beta > 1$, when the inner radius of the torus vanishes. When

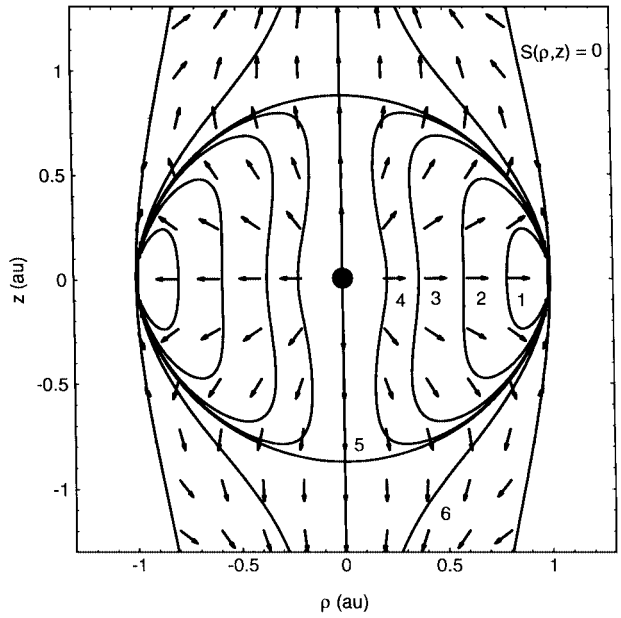

Fig. 2 Type II lightness number contours (see Table 1 for values).

Table 1 Solar sail lightness number and loading values for type II orbits

Contour	1	2	3	4	5	6
β	0.5	0.8	0.95	0.99	1.0	1.3
σ, gm^{-2}	3.06	1.91	1.61	1.55	1.53	1.18

$\beta = 1$, the surface is an oblate sphere with an infinite line along the z axis representing nonorbiting equilibrium solutions along the axis of rotation of the frame of reference. The nested tori intersect the ecliptic plane in a set of circular contours giving the required sail lightness number for 1-year orbits in the ecliptic plane. From Eq. (10a) it can be seen that in this case a radial sail attitude with zero pitch angle is required. Furthermore, along the z axis it can also be seen from Eqs. (10) that $\alpha = 0$ and $\beta = 1$, corresponding to an equilibrium solution at any distance along the axis of rotation of the frame of reference. In this simple equilibrium, the solar radiation-pressure acceleration is exactly balanced by the solar gravitational acceleration.

The region of space in the ρ–z plane in which displaced orbit solutions exist is bounded, being defined by the region interior to the surface $\hat{\boldsymbol{r}} \cdot \boldsymbol{n} = 0$. It can be seen from Eq. (8) that as this limiting surface is approached the sail lightness number $\beta \to \infty$. Using Eq. (6) it is found that the boundary is defined by

$$S(\rho, z; \omega) = (\mu/r) - \rho^2\omega^2 = 0 \tag{12}$$

where again $\omega = 1$ for the Earth-synchronous case. Inside the boundary surface $\hat{\boldsymbol{r}} \cdot \boldsymbol{n} > 0$ so that the solar radiation force can balance the sum of the gravitational and centripetal forces. However, outside the surface this balance cannot be achieved because $\hat{\boldsymbol{r}} \cdot \boldsymbol{n} < 0$. This corresponds to directing the solar radiation force toward the sun, which is clearly impossible. The surface $S = 0$ is shown as the outer contour in Fig. 2. Last, it should be noted that Earth-synchronous orbits near the Earth are perturbed by the Earth–moon system. Such three-body orbits have been previously investigated.[10]

Type III

To generate an optimal family of orbits, the solar sail orbit period will be treated as a free parameter with respect to which the sail lightness number may be minimized. Minimizing the sail lightness number reduces the required solar sail performance and so, for a fixed payload, will minimize the required sail area. Therefore, setting the derivative of β with respect to ω to zero in Eq. (10b), a quadratic in ω^2 is obtained, viz.,

$$\omega^4 - \omega^2\tilde{\omega}^2[2 + 3(z/\rho)^2] + \tilde{\omega}^4[1 + (z/\rho)^2] = 0 \tag{13}$$

This quadratic yields two solutions for ω^2, one of which fails to satisfy the condition $\hat{\boldsymbol{r}} \cdot \boldsymbol{n} \geq 0$, whereas the other solution always satisfies the condition. The solar sail orbital angular velocity required to provide the minimum sail lightness number is then given by

$$\omega = \tilde{\omega}\left[1 + \frac{3}{2}\left(\frac{z}{\rho}\right)^2\right]^{\frac{1}{2}}\left(1 - \left\{1 - \frac{1 + (z/\rho)^2}{\left[1 + \frac{3}{2}(z/p)^2\right]^2}\right\}^{\frac{1}{2}}\right)^{\frac{1}{2}} \tag{14}$$

It can be shown that the optimal family of orbits always requires a sail lightness number in the range $0 < \beta < 1$. Therefore, by treating ω as a free parameter of the problem, orbits with large out-of-plane displacements may be achieved with the required sail lightness number lower than for either of the type I or type II families. This is clearly a significant advantage, although the orbit period can no longer be chosen arbitrarily.

IV. Orbit Stability

Now that the families of displaced orbits have been reviewed, their linear stability characteristics will be investigated. This is achieved in the usual manner by linearizing the equations of motion about the nominal orbit solution to obtain a variational equation. The stability of the orbits may then be determined by examining the eigenvalues of the variational equation. It should be noted that only a linear analysis is performed, which in the present case provides necessary conditions for stability and sufficient conditions for instability.

The nonlinear equation of motion will be linearized by perturbing the sail from its nominal orbit with the sail attitude fixed in the rotating frame of reference. The perturbation is, therefore, applied with the sail elevation angle γ (as measured from the ecliptic plane) fixed, as shown in Fig. 1. The sail pitch angle α, therefore, varies due to the perturbation. First, a perturbation $\boldsymbol{\delta}$ will be added to the sail position vector at some point $\boldsymbol{r}_o = (\rho_o, \theta_o, z_o)$ on the nominal orbit such that $\boldsymbol{r}_o \to \boldsymbol{r}_o + \boldsymbol{\delta}$. Then, the variational equation is obtained from the nonlinear equation of motion as

$$\frac{\mathrm{d}^2\boldsymbol{\delta}}{\mathrm{d}t^2} + 2\boldsymbol{\omega} \times \frac{\mathrm{d}\boldsymbol{\delta}}{\mathrm{d}t} + \nabla U(\boldsymbol{r}_o + \boldsymbol{\delta}) - \boldsymbol{a}(\boldsymbol{r}_o + \boldsymbol{\delta}, \boldsymbol{n}) = 0 \tag{15}$$

where the vector $\boldsymbol{\delta}$ with components (ξ, ψ, η) represents first-order displacements in the rotating frame of reference in the (ρ, θ, z) directions, respectively. The potential gradient and the radiation-pressure acceleration may be expanded in Taylor series about the nominal orbit as

$$\nabla U(\boldsymbol{r}_o + \boldsymbol{\delta}) = \nabla U(\boldsymbol{r}_o) + \sum_{j=1}^{\infty} \frac{1}{j!}\left[\frac{\mathrm{d}^j}{\mathrm{d}\boldsymbol{r}^j}\nabla U(\boldsymbol{r})\right]_o \boldsymbol{\delta}^j \tag{16a}$$

$$\boldsymbol{a}(\boldsymbol{r}_o + \boldsymbol{\delta}, \boldsymbol{n}) = \boldsymbol{a}(\boldsymbol{r}_o, \boldsymbol{n}) + \sum_{j=1}^{\infty} \frac{1}{j!}\left[\frac{\partial^j}{\partial\boldsymbol{r}^j}\boldsymbol{a}(\boldsymbol{r}, \boldsymbol{n})\right]_o \boldsymbol{\delta}^j \tag{16b}$$

Retaining the first-order terms and noting that $\nabla U(\boldsymbol{r}_o) = \boldsymbol{a}(\boldsymbol{r}_o, \boldsymbol{n})$ along the nominal orbit, a linear variational equation with constant coefficients is obtained, viz.,

$$\frac{\mathrm{d}^2\boldsymbol{\delta}}{\mathrm{d}t^2} + \boldsymbol{S}\frac{\mathrm{d}\boldsymbol{\delta}}{\mathrm{d}t} + (\boldsymbol{M} - \boldsymbol{N})\boldsymbol{\delta} = 0 \tag{17}$$

where $\boldsymbol{M}$ and $\boldsymbol{N}$ are the gravity and radiation-pressure gradient matrices and $\boldsymbol{S}$ is the skew-symmetric gyroscopic matrix, given by

$$\boldsymbol{M} = \left[\frac{\mathrm{d}}{\mathrm{d}\boldsymbol{r}}\nabla U(\boldsymbol{r})\right]_o \tag{18a}$$

$$\boldsymbol{N} = \left[\frac{\partial}{\partial\boldsymbol{r}}\boldsymbol{a}(\boldsymbol{r}, \boldsymbol{n})\right]_o \tag{18b}$$

$$\boldsymbol{S} = \begin{bmatrix} 0 & -2 & 0 \\ 2 & 0 & 0 \\ 0 & 0 & 0 \end{bmatrix} \tag{18c}$$

The components of the matrices $\boldsymbol{M}$ and $\boldsymbol{N}$ are then the partial derivatives of the solar sail acceleration components with respect to the position coordinates. In component form the variational equation may be written as

$$\frac{\mathrm{d}^2\xi}{\mathrm{d}t^2} - 2\omega\rho_o\frac{\mathrm{d}\psi}{\mathrm{d}t} + L_{11}\xi + L_{13}\eta = 0 \tag{19a}$$

$$\frac{\mathrm{d}^2\psi}{\mathrm{d}t^2} + \frac{2\omega}{\rho_o}\frac{\mathrm{d}\xi}{\mathrm{d}t} = 0 \tag{19b}$$

$$\frac{\mathrm{d}^2\eta}{\mathrm{d}t^2} + L_{31}\xi + L_{33}\eta = 0 \tag{19c}$$

where $L_{ij} = M_{ij} - N_{ij}(i, j = 1\text{–}3)$. Because of the azimuthal symmetry of the problem all derivatives with respect to θ in the matrices $\boldsymbol{M}$ and $\boldsymbol{N}$ vanish. Therefore, the six terms $L_{2,j}$ and $L_{j,2}(j = 1\text{–}3)$ are zero. This set of three coupled, ordinary differential equations may be reduced to two by integrating Eq. (19b) to obtain

$$\frac{\mathrm{d}\psi}{\mathrm{d}t} = -\frac{2\omega}{\rho_o}(\xi - \xi_o) \tag{20}$$

This equation is in effect a linearized form of Kepler's third law, describing the orbital angular velocity of the solar sail relative to the nominal orbit due to the radial displacement ξ. Substituting Eq. (20) into Eq. (19a) then eliminates the azimuthal term. However, this substitution leads to a constant term $4\omega^2\xi_o$ in Eq. (19a) so that the variational equation is no longer homogeneous. It can be shown that the nonhomogeneity can be easily removed by rescaling the coordinates through a change of variable to

$$\tilde{\xi} = \xi - \frac{4\omega^2 L_{33}}{L_{11}L_{33} - L_{13}L_{31}}\xi_o \tag{21a}$$

$$\tilde{\eta} = \eta + \frac{4\omega^2 L_{13}}{L_{11}L_{33} - L_{13}L_{31}}\xi_o \tag{21b}$$

Using this transformation, a reduced variational system with a set of two coupled equations is then obtained, viz.,

$$\frac{\mathrm{d}^2}{\mathrm{d}t^2}\begin{bmatrix}\tilde{\xi}\\ \tilde{\eta}\end{bmatrix} + \begin{bmatrix}L_{11} & L_{13}\\ L_{31} & L_{33}\end{bmatrix}\begin{bmatrix}\tilde{\xi}\\ \tilde{\eta}\end{bmatrix} = \begin{bmatrix}0\\ 0\end{bmatrix} \tag{22}$$

It can be seen that by eliminating the azimuthal coordinate the order of the variational system is reduced from three to two. However, by ignoring the azimuthal motion it must be remembered that the solar sail is then free to drift along the nominal orbit. Therefore, orbit stability will be decided by determining if the motion in the ρ–z plane is bounded or unbounded.

By evaluating the partial derivatives along the nominal orbit, it is found that the coefficients of the matrix $\boldsymbol{L}$ are given by

$$L_{11} = 3\omega^2 + \tilde{\omega}^2\left[1 - 3\left(\frac{\rho}{r}\right)^2\right] + \frac{2\beta\tilde{\omega}^2}{r}\kappa\left(\frac{2\rho\kappa}{r^2} - \cos\gamma\right)\cos\gamma \tag{23a}$$

$$L_{13} = -3\tilde{\omega}^2\left(\frac{\rho z}{r^2}\right) + \frac{2\beta\tilde{\omega}^2}{r}\kappa\left(\frac{2z\kappa}{r^2} - \sin\gamma\right)\cos\gamma \tag{23b}$$

$$L_{31} = -3\tilde{\omega}^2\left(\frac{\rho z}{r^2}\right) + \frac{2\beta\tilde{\omega}^2}{r}\kappa\left(\frac{2\rho\kappa}{r^2} - \cos\gamma\right)\sin\gamma \tag{23c}$$

$$L_{33} = \tilde{\omega}^2\left[1 - 3\left(\frac{z}{r}\right)^2\right] + \frac{2\beta\tilde{\omega}^2}{r}\kappa\left(\frac{2z\kappa}{r^2} - \sin\gamma\right)\sin\gamma \tag{23d}$$

with the auxiliary coefficient κ defined as

$$\kappa = \rho\cos\gamma + z\sin\gamma \tag{23e}$$

The stability characteristics of the displaced orbits may now be investigated by calculating the eigenvalues of the variational equation. The eigenvalues may be obtained in the usual manner by substituting an exponential solution of the form

$$\begin{bmatrix}\tilde{\xi}\\ \tilde{\eta}\end{bmatrix} = \begin{bmatrix}\xi_o\\ \eta_o\end{bmatrix}\exp(\lambda t) \tag{24}$$

Substituting this solution into Eq. (22) yields a matrix equation of the form

$$\begin{bmatrix}\lambda^2 + L_{11} & L_{13}\\ L_{31} & \lambda^2 + L_{33}\end{bmatrix}\begin{bmatrix}\xi_o\\ \eta_o\end{bmatrix} = \begin{bmatrix}0\\ 0\end{bmatrix} \tag{25}$$

For nontrivial solutions a vanishing determinant of the matrix equation is required. This then yields the characteristic polynomial of the system as

$$f(\lambda^2) = \lambda^4 + \mathrm{tr}(\boldsymbol{L})\lambda^2 + \det(\boldsymbol{L}) = 0 \tag{26}$$

with the trace of the matrix $\mathrm{tr}(\boldsymbol{L}) = L_{11} + L_{33}$ and its determinant $\det(\boldsymbol{L}) = L_{11}L_{33} - L_{13}L_{31}$. The characteristic polynomial has four

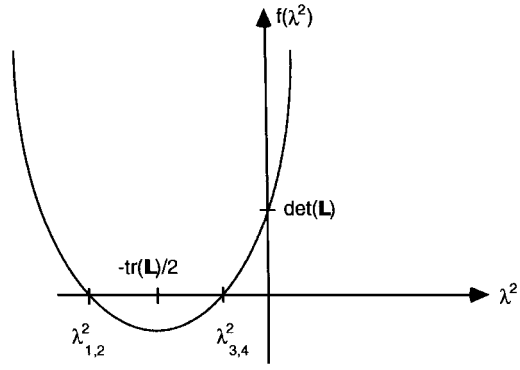

Fig. 3 Roots of the characteristic polynomial.

complex roots λ_j ($j = 1$–4), which represent the four eigenvalues of the system. Formally, these eigenvalues may be written as

$$\lambda_j = \left(\pm 1/\sqrt{2}\right)\left\{-\mathrm{tr}(\boldsymbol{L}) \pm [\mathrm{tr}(\boldsymbol{L})^2 - 4\det(\boldsymbol{L})]^{\frac{1}{2}}\right\}^{\frac{1}{2}} \tag{27}$$

where the negative root gives a long-period response and the positive root a short-period response. The sail motion in the neighbourhood of the nominal orbit is then given by the superposition of the four eigenmodes as

$$\begin{bmatrix}\tilde{\xi}\\ \tilde{\eta}\end{bmatrix} = \sum_{j=1}^{4}\begin{bmatrix}\xi_{oj}\\ \eta_{oj}\end{bmatrix}\exp(\lambda_j t) \tag{28}$$

The stability characteristics of the families of displaced orbits may now be investigated by searching for regions with purely imaginary eigenvalues, $\lambda_j^2 < 0$, ($j = 1$–4) giving stable, bounded oscillations in the ρ–z plane. For purely imaginary eigenvalues it is required that both $\det(\boldsymbol{L}) > 0$ and $\mathrm{tr}(\boldsymbol{L}) > 0$, as shown schematically in Fig. 3.

The stability characteristics of the family of type I orbits will be determined. Substituting for $\omega = \tilde{\omega}$ in Eqs. (23) it is found that

$$\mathrm{tr}(\boldsymbol{L}) = 4\tilde{\omega}^2(z/r)^2 \tag{29a}$$

$$\det(\boldsymbol{L}) = -\tilde{\omega}^4(\rho/r)^2 \tag{29b}$$

Therefore, because $\det(\boldsymbol{L}) < 0$ and $\mathrm{tr}(\boldsymbol{L}) > 0$, two of the eigenvalues will be positive and real, as can be seen from Fig. 3. It is, therefore, concluded that all type I orbits are unstable. The stability characteristics of the remaining two families of orbits can be investigated in a similar manner. However, clearer insight can be obtained by considering the family of type II orbits.

The stable region of the type II orbits will now be mapped with $\omega = 1$. Then, using the scale invariance of the problem, the stability of the type I and type III orbits can be seen. Setting $\omega = 1$ in Eqs. (23), it is found that there exists a stable family of orbits with $\lambda_j^2 < 0$, ($j = 1$–4) near the ecliptic plane. This region is bounded by the surface C_1, the section of which is shown in Fig. 4. The surface intersects the z axis at 0.794 AU corresponding to the maximum out-of-plane displacement for a stable type II orbit. It should be noted that the surface C_1 is not the same as the $\beta = 1$ contour in Fig. 2. In addition, it should also be noted that the z axis is not included in the set of stable orbits. Solutions along the z axis correspond to nonorbiting equilibrium solutions with solar radiation pressure balancing solar gravity.

For type I orbits the surface $\omega = 1$ is a unit sphere, the section of which is shown by the curve C_2 in Fig. 4. It can be seen that this surface lies outside the stable region of the map so that the $\omega = 1$ type I orbits will be unstable. This result has been confirmed by Eqs. (29). Furthermore, the surface defined by the $\omega = 1$ type III orbit, shown as the curve C_3 in Fig. 4, may also be generated and is found to lie within the stable region of the map. Therefore, all of the $\omega = 1$ type III orbits will be stable. It is found that the hierarchy of surfaces shown in Fig. 4 holds for any value of ω. The family of type I orbits are, therefore, always unstable, and the family of type III orbits are always stable, as can be confirmed numerically.

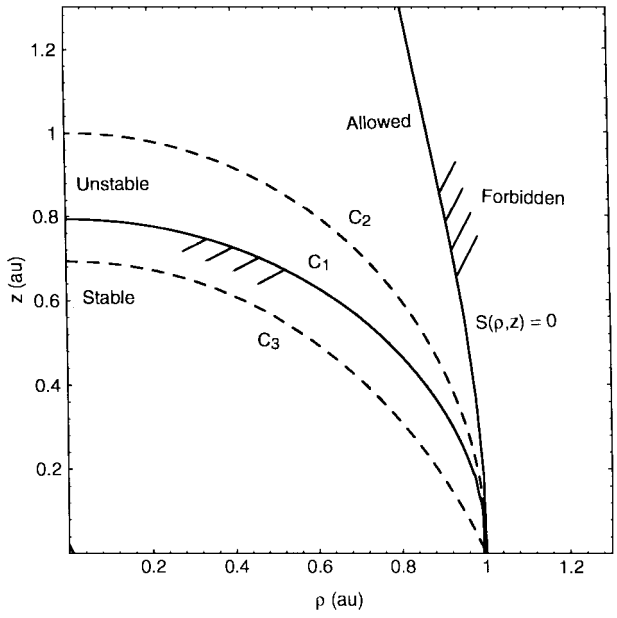

Fig. 4 Stable and unstable regions of the ρ–z plane.

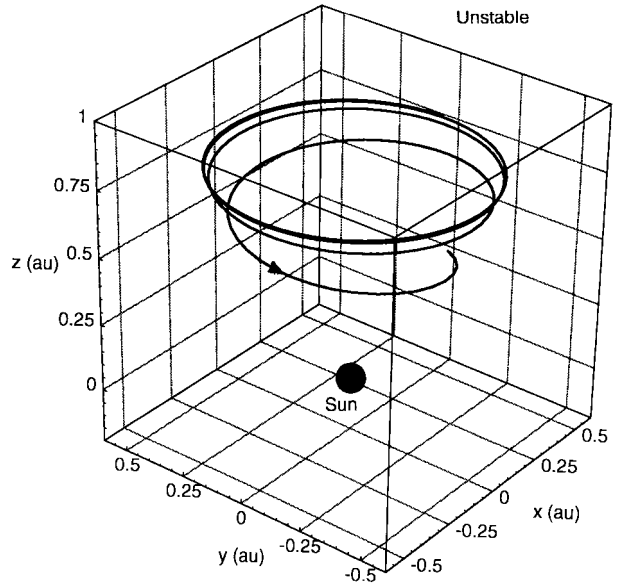

Fig. 5 Unstable 1-year type II orbit: $\rho_o = 0.5$ AU, and $z_o = 0.8$ AU.

As an example, a typical unstable response for a 1-year type II orbit is shown in Fig. 5 using numerical integration of the full nonlinear equations of motion. This unstable orbit has radius $\rho = 0.5$ AU and displacement $z = 0.8$ AU, which lie in the region of unstable type II orbits. It can be seen that the orbit has a rather long instability timescale, with the instability manifesting itself in the solar sail falling sunwards.

V. Orbit Control

The stability analysis of the last section has shown that some families of displaced orbits are unstable or have large regions of instability. Therefore, closed-loop control schemes that ensure stability will now be investigated. If the azimuthal position of the solar sail is unimportant, then the reduced two-dimensional variational equation may be used to investigate control laws that stabilize the motion in the ρ–z plane. It will be shown that the two-dimensional system is in principle controllable using state feedback to the sail pitch alone. This property is to be expected due to the coupling of the motion along the ρ and z axes.

Orbit Controllability

The first type of control to be investigated is proportional and derivative feedback to the sail elevation angle γ. However, it must first be established that the families of displaced orbits are in fact controllable using sail pitch alone. If the equation of motion is again linearized by allowing first-order changes in the sail position $\boldsymbol{r}_o \rightarrow \boldsymbol{r}_o + \boldsymbol{\delta}$ and also the sail attitude $\boldsymbol{n}_o \rightarrow \boldsymbol{n}_o + \delta\boldsymbol{n}$, such that $|\boldsymbol{n}_o + \delta\boldsymbol{n}| = 1$, a modified variational equation is then obtained, viz.,

$$\frac{\mathrm{d}^2\boldsymbol{\delta}}{\mathrm{d}t^2} + \boldsymbol{S}\frac{\mathrm{d}\boldsymbol{\delta}}{\mathrm{d}t} + (\boldsymbol{M} - \boldsymbol{N})\boldsymbol{\delta} = \boldsymbol{K}\delta\boldsymbol{n} \tag{30}$$

$$\boldsymbol{K} = \left[\frac{\partial}{\partial \boldsymbol{n}}\boldsymbol{a}(\boldsymbol{r}, \boldsymbol{n})\right]_o \tag{31}$$

where the matrix $\boldsymbol{K}$ gives the first-order variation in the solar radiation-pressure acceleration due to changes in the sail attitude. The azimuthal coordinate may again be eliminated using Eq. (20). Then, the coordinate transformations defined by Eqs. (21) may be used to reduce the variational equation to the variables $\tilde{\delta} = (\tilde{\xi}, \tilde{\eta})$. The variational equation then becomes

$$\frac{\mathrm{d}^2\tilde{\boldsymbol{\delta}}}{\mathrm{d}t^2} + \boldsymbol{L}\tilde{\boldsymbol{\delta}} = \boldsymbol{K}\delta\gamma \tag{32}$$

$$\boldsymbol{K} = \begin{bmatrix} \dfrac{\partial a_\rho}{\partial \gamma} \\ \dfrac{\partial a_z}{\partial \gamma} \end{bmatrix} \tag{33}$$

where the first-order attitude change $\delta\boldsymbol{n}$ now becomes the change in the sail elevation angle $\delta\gamma$. The radiation-pressure acceleration partial derivatives, given by the components of $\boldsymbol{K} = (K_1, K_2)^T$, are found to be

$$K_1 = (\beta z/2r^4)(\rho\cos\gamma + z\sin\gamma) \times \{3\cos 2\gamma[1 - (\rho/z)\tan 2\gamma] + 1\} \tag{34a}$$

$$K_2 = (\beta\rho/2r^4)(\rho\cos\gamma + z\sin\gamma) \times \{3\cos 2\gamma[1 + (z/\rho)\tan 2\gamma] - 1\} \tag{34b}$$

The variational equation may now be written in standard state-space form using a state variable $\boldsymbol{x} = (\tilde{\delta}, \mathrm{d}\tilde{\delta}/\mathrm{d}t)$, viz.,

$$\frac{\mathrm{d}\boldsymbol{x}}{\mathrm{d}t} = \boldsymbol{L}^*\boldsymbol{x} + \boldsymbol{K}^*\delta\gamma \tag{35a}$$

$$\boldsymbol{L}^* = \begin{bmatrix} \boldsymbol{0} & \boldsymbol{I} \\ -\boldsymbol{L} & \boldsymbol{0} \end{bmatrix} \tag{35b}$$

$$\boldsymbol{K}^* = \begin{bmatrix} \boldsymbol{0} \\ \boldsymbol{K} \end{bmatrix} \tag{35c}$$

To determine the controllability of the system, the rank of the 4×4 controllability matrix $\boldsymbol{C} = [\boldsymbol{K}^*, \boldsymbol{L}^*\boldsymbol{K}^*, \boldsymbol{L}^{*2}\boldsymbol{K}^*, \boldsymbol{L}^{*3}\boldsymbol{K}^*]$ will be calculated from the system matrix $\boldsymbol{L}^*$ and the input matrix $\boldsymbol{K}^*$. For the system to be fully controllable the matrix $\boldsymbol{C}$ must have full rank. Evaluating the controllability matrix it is found that

$$\boldsymbol{C} = \begin{bmatrix} 0 & K_1 & 0 & -L_{11}K_1 - L_{13}K_2 \\ 0 & K_2 & 0 & -L_{31}K_1 - L_{33}K_2 \\ K_1 & 0 & -L_{11}K_1 - L_{13}K_2 & 0 \\ K_2 & 0 & -L_{31}K_1 - L_{33}K_2 & 0 \end{bmatrix} \tag{36}$$

Then, for the controllability matrix to have full rank, its determinant must be nonzero. Therefore, after some reduction the determinant is found to be

$$\det(\boldsymbol{C}) = -[K_1(L_{31}K_1 + L_{33}K_2) - K_2(L_{11}K_1 + L_{13}K_2)]^2 \tag{37}$$

The controllability of the family of type I orbits will be considered. Substituting for $\omega = \tilde{\omega}$ in Eq. (37) it is found that

$$\det(\boldsymbol{C}) = -\frac{64\tilde{\omega}^{12}\rho^6 z^2}{r^2}\left[1 - \frac{7}{8}\left(\frac{z}{\rho}\right)^2\right]^2 \tag{38}$$

Therefore, the family of type I orbits is in general controllable using state feedback to the sail elevation angle alone. From Eq. (38) it can be seen that the only uncontrollable subset of orbits are those satisfying

$$z = \sqrt{\tfrac{8}{7}}\rho \tag{39}$$

However, this uncontrollable subset is not problematic as Eq. (39) represents an exact equality that can be avoided in practice. In general it is found that $\det(\boldsymbol{C})$ is nonzero for the other orbit families so that state feedback to the sail elevation angle can ensure asymptotic stability in the ρ–z plane. Again, such controllability is to be expected as the motion in the ρ and z axes is strongly coupled through the matrix $\boldsymbol{L}$.

Active Control

Now that the controllability of the families of displaced orbits has been established, a closed-loop control law using the sail elevation angle will be investigated. The sail elevation angle will be related to the state variables through a general feedback expression of the form

$$\delta\gamma = \sum_{j=1}^{4} g_j x_j \tag{40}$$

where x_j ($j = 1$–4) are the four components of the state vector $\boldsymbol{x}$. The four feedback gains g_j ($j = 1$–4) are then chosen to ensure that all four of the eigenvalues of the system lie in the left-hand complex plane so that the system has asymptotic stability. Because the reference state of the system is $\boldsymbol{x} = 0$, the controller is a state regulator. Equation (40) can now be substituted into Eq. (32) and a new characteristic polynomial obtained. The gains may then be selected in any suitable manner, such as the root locus technique. The closed-loop response of the controller is shown in Fig. 6 for the same unstable type II orbit considered in Sec. IV. It can be seen from Fig. 7 that only small trims to the sail elevation angle are required to ensure stability. However, the damping timescale is rather long due to the coupling between the magnitude and direction of the solar radiation pressure force.

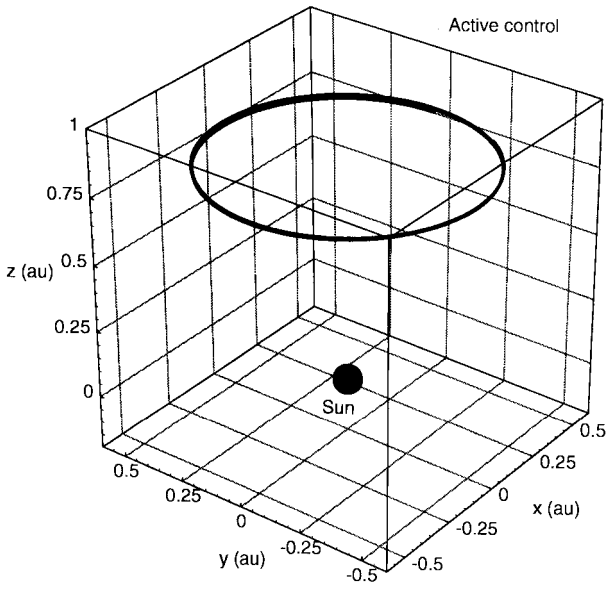

Fig. 6 Active control of an unstable type II orbit: $\xi_o = 10^{-2}\rho_o$ and $\eta_o = 10^{-2} z_o$.

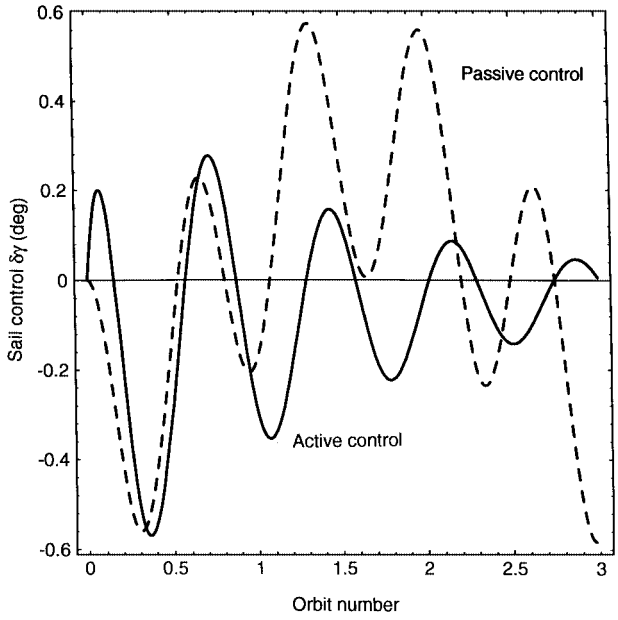

Fig. 7 Sail elevation angle time history.

Passive Control

An extremely simple closed-loop scheme will now be investigated that ensures stability for all of the families of displaced orbits. The control scheme does not possess active damping but is used only to ensure that unstable orbits, such as 1-year type II orbits high above the ecliptic plane, remain bounded. The scheme requires only that the sail pitch angle α remains fixed in the rotating frame of reference. Therefore, as the sail moves away from the nominal orbit, the sail elevation angle γ must vary to maintain the fixed pitch angle. The sail pitch angle can be fixed by designing the solar sail to be slightly conical in shape with the apex of the cone directed toward the sun. Such a conical shape maintains a sun-facing attitude by developing restoring torques if the sail is rotated away from the sun. A nonzero pitch angle can be maintained by a suitable offset of the center of mass from the center of pressure. Such passive attitude stabilization has been discussed in detail elsewhere.[11,12]

For a fixed sail pitch angle, the components of the solar radiation-pressure acceleration (a_ρ, a_z) may be written as

$$a_\rho = (\beta/r^2)\cos^2\alpha[\cos\alpha(\rho/r) - \sin\alpha(z/r)] \tag{41a}$$

$$a_z = (\beta/r^2)\cos^2\alpha[\sin\alpha(\rho/r) - \cos\alpha(z/r)] \tag{41b}$$

These expressions may then be expanded to first order in a Taylor series and a new system matrix formed. It is found that the reduced variational equation now becomes

$$\frac{\mathrm{d}^2}{\mathrm{d}t^2}\begin{bmatrix}\tilde{\xi}\\ \tilde{\eta}\end{bmatrix} + \begin{bmatrix}P_{11} & P_{13}\\ P_{31} & P_{33}\end{bmatrix}\begin{bmatrix}\tilde{\xi}\\ \tilde{\eta}\end{bmatrix} = \begin{bmatrix}0\\ 0\end{bmatrix} \tag{42}$$

where the coefficients of the matrix $\boldsymbol{P}$ are given by

$$P_{11} = 3\tilde{\omega}^2 + \tilde{\omega}^2[1 - 3(\rho/r)^2] + 3\beta\tilde{\omega}^2\cos^2\alpha(\rho/r)\kappa_1 - \beta\tilde{\omega}^2\cos^3\alpha \tag{43a}$$

$$P_{13} = -3\tilde{\omega}^2(\rho z/r^2) + 3\beta\tilde{\omega}^2\cos^2\alpha(z/r)\kappa_1 + \beta\tilde{\omega}^2\cos^2\alpha\sin\alpha \tag{43b}$$

$$P_{31} = -3\tilde{\omega}^2(\rho z/r^2) + 3\beta\tilde{\omega}^2\cos^2\alpha(\rho/r)\kappa_2 - \beta\tilde{\omega}^2\cos^2\alpha\sin\alpha \tag{43c}$$

$$P_{33} = \tilde{\omega}^2[1 - 3(z/r)^2] + 3\beta\tilde{\omega}^2\cos^2\alpha(z/r)\kappa_2 - \beta\tilde{\omega}^2\cos^3\alpha \tag{43d}$$

with the auxiliary coefficients κ_1 and κ_2 defined by

$$\kappa_1 = (1/r)(\rho\cos\alpha - z\sin\alpha) \tag{43e}$$

$$\kappa_2 = (1/r)(\rho\sin\alpha + z\cos\alpha) \tag{43f}$$

To determine the linear stability of this system, a new characteristic polynomial is formed and the eigenvalues of the system found, viz.,

$$\omega^4 + \mathrm{tr}(\boldsymbol{P})\omega^2 + \det(\boldsymbol{P}) = 0 \tag{44}$$

The conditions for purely imaginary eigenvalues, and hence stability, are again that $\mathrm{tr}(\boldsymbol{P}) > 0$ and $\det(\boldsymbol{P}) > 0$. However, due to the hierarchy of stability, as discussed in Sec. IV, only the stability characteristics of the type I orbit family need be examined. Substituting for $\omega = \tilde{\omega}$ in Eqs. (43), it is found that

$$\mathrm{tr}(\boldsymbol{P}) = \tilde{\omega}^2[2 + (z/r)^2] \tag{45a}$$

$$\det(\boldsymbol{P}) = \tilde{\omega}^4(\rho/r)^2 \tag{45b}$$

both of which are clearly positive. It can be seen then that the family of type I orbits is rendered stable using the simple fixed sail pitch angle control. Therefore, using a similar argument to that discussed in Sec. IV, it can be shown that all other families of displaced orbits are rendered linearly stable, as can be confirmed numerically.

The required change in the sail elevation angle $\delta\gamma$ can be written as a state feedback law by evaluating the change in sail pitch angle with first-order changes in ρ and z. The sail pitch angle α may be written as

$$\alpha = \gamma - \tan^{-1}(z/\rho) \tag{46}$$

so that the required control law to maintain a fixed sail pitch angle is then $\delta\gamma = -\delta\alpha$, viz.,

$$\delta\gamma = \frac{1}{\rho}\frac{1}{1 + (z/\rho)^2}\left[\eta - \frac{z}{\rho}\xi\right] \tag{47}$$

In state feedback form the equivalent gains are, therefore,

$$g_1 = -\frac{1}{\rho}\frac{z/\rho}{1 + (z/\rho)^2} \tag{48a}$$

$$g_2 = \frac{1}{\rho}\frac{1}{1 + (z/\rho)^2} \tag{48b}$$

$$g_3 = 0 \tag{48c}$$

$$g_4 = 0 \tag{48d}$$

The performance of the controller is shown in Fig. 8, again using the unstable type II orbit considered in Sec. IV. As can be seen, the orbit is now stable although there is no active damping of the modes of oscillation of the orbit. Again, only small trims to the sail elevation angle are required, as shown in Fig. 7. This simple control scheme is clearly appealing because in principle no state variable information is required. For active control of the sail attitude a sun sensor would measure the change in sail pitch angle $\delta\alpha$, which would then be used directly to command an opposite change in sail elevation angle $\delta\gamma$. Alternatively, for passive control of the sail attitude, the sail pitch angle is held constant by restoring torques generated by the sail shape so that all families of orbits are rendered naturally stable. It is this inherent simplicity that makes the control law both attractive and interesting.

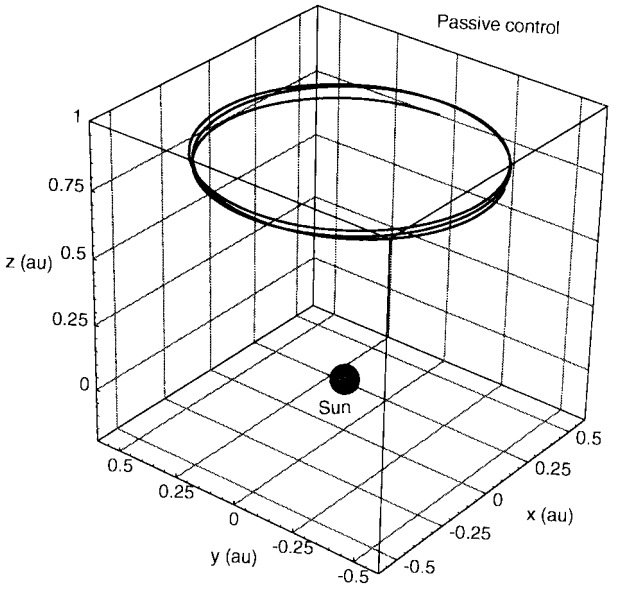

Fig. 8 Passive control of an unstable type II orbit: $\xi_o = 10^{-2}\rho_o$ and $\eta_o = 10^{-2}z_o$.

VI. Conclusions

The existence and stability of families of displaced solar sail orbits have been reviewed. It has been be demonstrated that the unstable subset of orbits are in general controllable using state feedback to the sail elevation angle alone. Then, a passive control scheme has been presented that renders the unstable subset of orbits linearly stable. This passive control scheme requires only that the sail attitude is held fixed relative to the sun. Such a fixed attitude can in principle be achieved passively with a conical sail and a suitable offset of the center of mass from the center of pressure. Therefore, due to its inherent simplicity, the passive control scheme appears to be an attractive means of orbit stabilization.

Appendix: Solar Sail Lightness Number

The performance of a solar sail can be characterized by the sail lightness number β. In this section the relationship between the lightness number and mass per unit area σ will be derived. The solar energy flux F_S at distance r from the sun is given by

$$F_S = L_S/4\pi r^2 \tag{A1}$$

where $L_S(3.826 \times 10^{26}\ \mathrm{Js}^{-1})$ is the solar luminosity. Then, the pressure P exerted on a perfectly reflecting solar sail is $2F_S/c$, where c $(3 \times 10^8\ \mathrm{ms}^{-1})$ is the speed of light. For a solar sail of mass m and area A, the acceleration due to solar radiation pressure is, therefore,

$$a_R = \frac{L_S}{2\pi c r^2}\frac{A}{m} \tag{A2}$$

Similarly, the acceleration due to solar gravity is given by

$$a_G = GM_S/r^2 \tag{A3}$$

where $M_S(1.99 \times 10^{30}\ \mathrm{kg})$ is the solar mass and $G(6.67 \times 10^{-11}\ \mathrm{Nm^2\ kg^{-2}})$ is the universal gravitational constant. Therefore, by definition, the lightness number may be written as the ratio a_S/a_G, viz.,

$$\beta = \frac{L_S}{2\pi G M_S c}\frac{1}{\sigma} \tag{A4}$$

where σ is the solar sail mass per unit area m/A. Substituting for the appropriate constants just listed, it is found that

$$\beta = \frac{1.529}{\sigma}(\mathrm{gm}^{-2}) \tag{A5}$$

Using aluminized plastic film a sail lightness number of order 0.5–0.8 may be possible with minimal payload. However, a high-performance sail with a lightness number ≥ 1 would require an all-metal film.[9]

References

[1]McInnes, C. R., and Simmons, J. F. L., "Halo Orbits for Solar Sails—Dynamics and Applications," *European Space Agency Journal*, Vol. 13, No. 3, 1989, pp. 229–234.

[2]McInnes, C. R., and Simmons, J. F. L., "Halo Orbits for Solar Sails I: Heliocentric Case," *Journal of Spacecraft and Rockets*, Vol. 29, No. 4, 1992, pp. 466–471.

[3]McInnes, C. R., and Macpherson, K. P., "Solar Sail Halo Trajectories: Dynamics and Applications," 42nd International Astronautical Congress, International Astronautical Federation Paper 91-334, Montreal, PQ, Canada, Oct. 1991.

[4]McInnes, C. R., "Advanced Trajectories for Solar Sail Spacecraft," Ph.D Thesis, Dept. of Physics and Astronomy, Univ. of Glasgow, Glasgow, Scotland, UK, Oct. 1991.

[5]Mashkevich, S. V., and Shvartsburg, A. A., "Best Solar Sail for Heliocentric Halos," *Soviet Physics Doklady*, Vol. 37, No. 6, 1992, pp. 290–293.

[6]Molostov, A. A., and Shvartsburg, A. A., "Heliocentric Halos for a Solar Sail with Absorption," *Soviet Physics Doklady*, Vol. 37, No. 3, 1992, pp. 149–152.

[7]Molostov, A. A., and Shvartsburg, A. A., "Heliocentric Synchronous Halos for a Solar Sail with Absorption," *Soviet Physics Doklady*, Vol. 37, No. 4, 1992, pp. 195–197.

[8]McInnes, C. R., and Brown, J. C., "The Dynamics of Solar Sails with a Non-Point Source of Radiation Pressure," *Celestial Mechanics and Dynamical Astronomy*, Vol. 49, No. 3, 1990, pp. 249–264.

[9]Wright, J. L., *Space Sailing*, Gordon and Breech Science, Philadelphia, PA, 1992, pp. 1–3.

[10]McInnes, C. R., McDonald, A. J. C., Simmons, J. F. L., and MacDonald, E. W., "Solar Sail Parking in Restricted Three-Body Systems," *Journal of Guidance, Control, and Dynamics*, Vol. 17, No. 2, 1994, pp. 399–406.

[11]Sohn, R., "Attitude Stabilisation by Means of Solar Radiation Pressure," *ARS Journal*, Vol. 29, No. 5, 1959, pp. 371–373.

[12]Kirpichnikov, S. N., Kirpichnikova, E. S., Polyakhova, E. N., and Shmyrov, A. S., "Planar Heliocentric Roto-translational Motion of a Spacecraft with a Solar Sail of Complex Shape," *Celestial Mechanics and Dynamical Astronomy*, Vol. 63, No. 3, 1996, pp. 255–269.